A Langevin equation for the energy cascade in fully-developed turbulence.

Philippe Marcq [a] and Antoine Naert [b]

[a] *Department of Physics, Graduate School of Science, Kyoto University, Kyoto 606, Japan*

[b] *Laboratoire de Physique, Ecole Normale Supérieure de Lyon, 46 Allée d'Italie, 69394 Lyon Cédex 07, France*

Abstract

Experimental data from a turbulent jet flow is analysed in terms of an additive, continuous stochastic process where the usual time variable is replaced by the scale. We show that the energy transfer through scales is well described by a linear Langevin equation, and discuss the statistical properties of the corresponding random force in detail. We find that the autocorrelation function of the random force decays rapidly: the process is therefore Markov for scales larger than Kolmogorov's dissipation scale η. The corresponding autocorrelation scale is identified as the elementary step of the energy cascade. However, the probability distribution function of the random force is both non-Gaussian and weakly scale-dependent.

PACS numbers: 47.27.Gs, 47.27.Jv, 05.40.+j

1 Introduction

Due to the molecular viscosity of the fluid, the kinetic energy of a flow must be dissipated. The degree of instability of a flow is usually quantified by the Reynolds number Re, defined as $Re = UL/\nu$ where U, L and ν are respectively the mean velocity, the largest scale of the flow, and the kinematic viscosity of the fluid. For large enough Reynolds number, the dissipation scale η at which energy is dissipated becomes much smaller than the integral scale L at which it is injected: $L \gg \eta$. The transport process through which energy injected at large scale is transported down to small scales is traditionally referred to as a "cascade", following Richardson's qualitative picture of turbulent eddies breaking down into smaller sub-eddies from the largest scales of motion down to the dissipative scales [1,2].

Richardson's ideas were first made quantitative by Kolmogorov [3]. Kolmogorov's theory underlines the central role plaid by the mean energy dissipation rate $\langle\epsilon\rangle$. Its main assumptions are that, for sufficiently large Reynolds number, (i) small scale turbulence (i.e. $r \ll L$) is homogeneous and isotropic, and thus decoupled from the large-scale properties of the flow, which may be affected by, e.g., the specific geometry of boundary conditions; (ii) for scales large compared to the dissipation scale ($r \gg \eta$), $\langle\epsilon\rangle$ is independent of ν. Whenever (i) and (ii) hold, one expects small scale statistical properties of the cascade process to be universal, and determined only by $\langle\epsilon\rangle$ in the inertial range $\eta \ll r \ll L$. In addition, dimensional arguments lead to a simple scaling form for the probability distribution function of velocity increments. This theory becomes inconsistent if one allows the energy dissipation rate to fluctuate. However, experimental data shows unambiguously that the Kolmogorov picture is incomplete [1,2]: the energy dissipation rate ϵ is a strongly fluctuating quantity. Its inhomogeneous, intermittent behaviour effectively links small and large-scale features of the flow. Further, the probability distribution function of velocity increments is not scale-invariant: its shape is Gaussian at large scale, yet develops long tails at smaller scale.

The first phenomenological model to take into account the strong variability of the energy dissipation rate was proposed by Kolmogorov and Obukhov [4]. In this picture, emphasis is shifted from $\langle\epsilon\rangle$ to the local average ϵ_r integrated over a ball of radius r. The fluctuations of the random variable $\ln\epsilon_r$ are assumed to be Gaussian:

$$P(\ln\epsilon_r, r) = \frac{1}{\Lambda(r)\sqrt{2\pi}}\ \exp\left(-\frac{\left(\ln\epsilon_r - \langle\ln\epsilon_r\rangle\right)^2}{2\Lambda^2(r)}\right). \qquad (1)$$

Further, the variance $\Lambda^2(r)$ depends logarithmically on scale:

$$\Lambda^2(r) = \Lambda_0^2 + \mu\ln(L/r), \qquad (2)$$

where μ is a constant and Λ_0 accounts for the large scale properties of the flow. Log-normal probability distribution functions (Eq. (1)) are known to be a good first-order approximation of the statistics of the energy transfer rate in fully-developed turbulent flows [5,6]. They arise naturally as solutions of multiplicative stochastic processes for the variable ϵ_r [7,8], where interaction is generally assumed to be local in scale: the stochastic process must be Markov. However, this assumption is generally not verified by experimental data [9]. Approaches related to the log-normal model (Eqs. (1-2)) have attracted renewed attention recently [10,11], despite well-known difficulties linked to the scaling properties of ϵ_r and of the velocity increments δv_r. [8,12].

The statistical properties of isotropic and homogeneous turbulent flows have

been reconsidered recently within the context of continuous, additive, Markov stochastic processes [13,14]. Analysis of experimental data from a turbulent flow has shown that the scale-dependence of probability distribution functions of velocity increments [13] and of the logarithm of the energy dissipation rate [14] may be described by Fokker-Planck equations, where the usual time variable is replaced by a monotonous function of scale r. The energy cascade corresponds to an Ornstein-Uhlenbeck process for the stochastic variable $\ln \epsilon_r$, since the drift and diffusion terms of the Fokker-Planck equation are respectively found linear and constant. This model is exactly solvable. The probability distribution function is found Gaussian: the statistics of ϵ_r are log-normal. However, the scale-dependence of the mean and variance differs from that considered in previously studied log-normal models [4,10]. The presence of a non-zero drift term implies that this new phenomenological approach is not equivalent to usual multiplicative models for the variable ϵ_r.

In this work, we consider an alternative formulation of the model introduced in [14]. Our analysis is based on the same velocity signal, recorded in a low-temperature turbulent jet flow at high Reynolds number $Re = 20000$. We aim at building a faithful, yet simple model of available experimental data, from a phenomenological perspective. Fokker-Planck equations, which govern the evolution of probability distribution functions, are equivalent mathematically to stochastic differential equations with an additive noise term (Langevin equations, see [15]). The goal pursued here is to investigate the energy transfer process from the complementary viewpoint given by stochastic trajectories in scale. A detailed study of statistical quantifiers which arise naturally in this new context allows to check the overall consistency of the approach. In particular, the validity of approximations made in [14] is investigated in detail.

This article is organised as follows. The experimental set-up is discussed in Sec. 2, together with the specifics of data acquisition and signal processing. Prescriptions used in the analysis of the experimental velocity signal are introduced in Sec. 3. The results previously obtained in [14] are summarised in Sec. 4. The stochastic cascade process is next examined in detail within the context of a Langevin description in Sec. 5. The Markov and Gaussian nature of the process are then discussed in Secs. 6 and 7 respectively. Sec. 8 is devoted to a summary and discussion of our results.

2 A low-temperature jet flow

The velocity signal analysed in this work was recorded in a low-temperature gaseous helium jet flow [16–18]. Experimental conditions (temperature $T = 4.2$ K, pressure $P = 1$ bar) are set close to the liquid-gas transition: this ensures a very low kinematic viscosity, $\nu \simeq 2 \times 10^{-8}$ m^2 s^{-1}, and thus gives access to

high Reynolds numbers, up to $Re \sim 10^5$ in this cell.

After laminarisation, gaseous helium is injected through a contracting nozzle (diameter 2 mm) into a cylindrical cell (diameter 13 cm, height 30 cm) where the turbulent jet develops. A grid is set 17 cm downstream from the nozzle to avoid instability occurring on long time scales due to recirculation of the flow along the walls. Further downstream, gaseous helium is pumped out of the cryostat. Adjusting the microvalve inlet opening and the outlet pumping allows to vary not only the flow rate (mean velocity U), but also the operating pressure P in the cell. Since the product $P\nu$ is roughly constant, this original feature of the experiment allows to vary the Reynolds number over the range $10^3 \leq Re \leq 10^5$. Access to a large range of Reynolds number for a fixed geometry is the main benefit of this cryogenic experiment (see [18] for further details).

The longitudinal component of the velocity is measured thanks to a cryogenic hot-wire anemometer [17] located 10 cm downstream from the nozzle on the axis of the jet, where the flow is fully turbulent. The effective spatial resolution is estimated to be 22μm. The wire is operated at constant resistance through a home-made 10 MHz lock-in amplifier. The signal is next digitalised using a 12 bits A/D converter. We believe that the dominant source of experimental error is the resolution of the digitalization.

What represents, from a physical point of view, the signal recorded by the hot wire? The velocity field is a function of space and time $v(x,t)$. In a jet geometry, as in many experimental flows, the turbulent velocity field is advected relatively to the observer (anemometer). The "rate of velocity fluctuations" is ususally defined as the ratio of the standard deviation of the velocity over its mean value. A small value of this rate means that the flow is effectively "frozen": Taylor's frozen turbulence hypothesis is valid [1]. Rapid advection of the velocity field $v(x,t)$ with respect to the (fixed) detector ensures that the signal records the spatial structure of the velocity field ($v(x,t) \simeq v(x)$, with $x = \langle v \rangle t$), rather than its temporal evolution. In this jet, the rate of fluctuation is 28%, in agreement with values typical of jet flows. The frozen turbulence hypothesis is now a source of error [19], in fact a bias on estimates of the spatial velocity field $v(x)$.

In the present work, this point is taken into account by resampling the signal as follows (see [20] for further details). The spatial coordinate x of a record taken at time t is $x(t) = \int_0^t v(t)dt$. The bias on the velocity signal can be eliminated by considering instead the series $v(x(t))$. However, the interval between two successive points becomes irregularly distributed. One must also resample the signal regularly, in practice by linear interpolation. We checked that a more precise interpolation, involving the second order derivative, does not sensibly improve the regularity of sampling, and leaves our measurements unchanged.

Moreover, our conclusions do not seem to depend on the choice of a specific correction method, since results remain unchanged when using, e.g., the local Taylor hypothesis advocated in [19].

For consistency, the velocity signal we analyse is the same as studied in [14], and was recorded at $Re = 20000$. The Reynolds number based on Taylor's microscale is $R_\lambda = 341$. The dissipation scale is estimated to $\eta = 20\mu$m according to Kolmogorov's formula:

$$\eta = \left(\frac{\nu^3}{\langle \epsilon \rangle} \right)^{1/4}, \tag{3}$$

with $\langle \epsilon \rangle$ defined as $15\nu \ \langle \ (\mathrm{d}v/\mathrm{d}x)^2 \ \rangle$. The smallest structure of the flow is therefore resolved at this value of Re: this justifies our choice of this specific sample. The integral scale, operationally defined as the correlation length of the velocity signal, is evaluated to $L \simeq 1$ cm ($L \simeq 500\eta$). This numerical value indeed corresponds to the largest structure of the flow, since the diameter of the jet is about 2.5 cm in the vicinity of the anemometer, where the measurement is done. Note however that the values of η and L only have qualitative importance in our study.

3 Prescriptions for data analysis

As proposed by Obukhov [4], the dissipation averaged over a volume of size r may be used as a reasonable Ansatz for the local transfer rate of energy at scale r. Since available experimental data is often limited to the longitudinal velocity component $v(x)$, it is customary to use the following one-dimensional surrogate of the dissipation $\epsilon_r(x)$ at location x:

$$\epsilon_r(x) = \frac{15\nu}{r} \int_{x-r/2}^{x+r/2} \left(\frac{dv}{dx'} \right)^2 dx', \tag{4}$$

a definition which we endorse here. Eq. (4) is generally believed to capture most of the relevant physics (see [2] for up-to-date critical overviews).

Even though the relevant physics is continuous, experimental data has been sampled before being recorded: the available data is thus discrete, with a sampling distance equal to $d = 22\mu$m (or $d = 1.1\eta$). In what follows, the unit of length is set to d unless otherwise noted. Values of the dissipation field $\epsilon_r(x)$ are obtained thanks to a first-order finite-difference approximation of

the derivative of the velocity field:

$$\epsilon_r(x) = \frac{15\nu}{r} \sum_{x'=x-\mathrm{int}(r/2)}^{x+\mathrm{int}(r/2)-1} \left(\frac{v\,(x'+\delta x') - v(x')}{\delta x'} \right)^2 , \tag{5}$$

where $\delta x'$ is the (constant) discretisation step. The numerical value:

$$\delta x' = 5, \tag{6}$$

is adopted in all calculations reported here. Note that with this choice, the fluctuations of ϵ_r at $r \simeq \eta$ cannot be resolved since $\delta x' = 5.5\eta$.

In the following, we will refer to both variables r and l as "scale", where the new variable l is related to the physical scale r (as used in Eq. (4)) by :

$$l = \ln\left(\frac{L}{r}\right). \tag{7}$$

This definition is used for convenience since it leads to simpler analytic expressions. For the relevant scales $\eta \leq r \leq L$, the continuous variable l is positive and bounded from above:

$$0 \leq l \leq \ln\left(\frac{L}{\eta}\right) \tag{8}$$

It is a monotonously decreasing function of the usual scale r. For clarity, scale will however be measured in units of the dissipation scale η in most graphs.

The random process $X(l)$ is defined as:

$$X(l) = \ln \epsilon_r, \tag{9}$$

using Eqs. (4) and (7). Statistical averages, denoted by the symbol $\langle\ \rangle$, are evaluated over the whole data set (10^7 points, or about $2\ 10^4 L$). For all statistical quantifiers presented here, this set is large enough to ensure statistical convergence, as confirmed by comparisons with results obtained from smaller samples.

For convenience, we will also consider the centered variable $Y(l)$, defined by:

$$Y(l) = X(l) - \langle X(l) \rangle. \tag{10}$$

The probability distribution functions $P(Y, r)$ of the variable $Y(r)$ computed according to Eq. (5) are shown in Fig. 1. Despite rough agreement with the

parabolic shape expected for a Gaussian distribution in a lin-log plot, an obvious departure from the functional form (1) is the asymmetry of $P(Y,r)$. This point has already been noted in previous experimental [5] and numerical work [6].

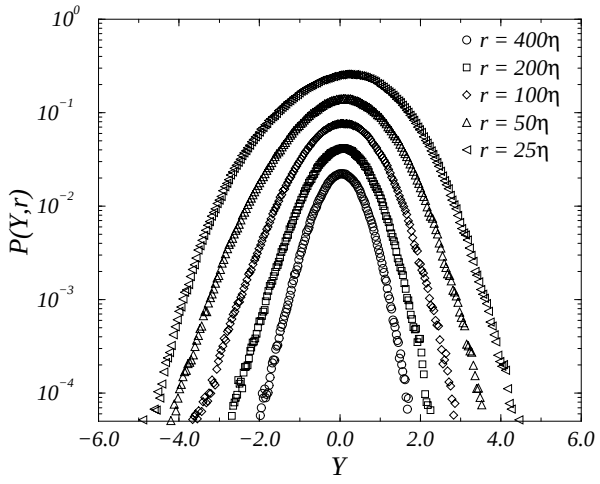

Fig. 1. Probability distribution functions $P(Y,r)$ of the centered variable Y at scales r ranging from $r = 25\eta$ to 400η. The variance $\langle Y(r)^2 \rangle$ is a decreasing function of scale. Asymmetry of the histograms translates into a non-zero value of the skewness. For clarity, histograms were shifted by a factor 2 along the vertical axis.

Evaluation of the scale-derivative of $Y(l)$ will also be needed in the following. A first-order approximation will be used:

$$\frac{\mathrm{d}Y}{\mathrm{d}l}(l) = \frac{1}{\delta l} \left(Y\left(l + \delta l\right) - Y(l) \right); \tag{11}$$

where the step δl is naturally related to the physical scale difference δr by the relation:

$$\delta l(r) = \ln \left(\frac{r + \delta r}{r} \right). \tag{12}$$

We use here the numerical value:

$$\delta r = 4, \tag{13}$$

or $\delta r = 4.4\eta$. The discretisation step is thus a decreasing function of physical scale r: $\delta l(r = 25\eta) \sim 0.17$, $\delta l(r = 100\eta) \sim 0.04$, $\delta l(L) \sim 0.009$. Our results are unchanged for other reasonable numerical values of the discretisation steps (6) and (13). This ensures that the continuous limit is well-controlled.

4 An Ornstein-Uhlenbeck process

In this section, we wish to summarise the analysis made in [14] of the stochastic process $X(l)$, as defined above.

A first important result is that the transition probability distribution function $P\left(X', l'|X, l\right) = P\left(X(l')|X(l)\right)$ respects the Chapman-Kolmogorov equation to a very good approximation. Mathematically, the Chapman-Kolmogorov equation is a necessary (but not sufficient) condition for the process to be Markov. An equivalent (differential) formulation is the Kramers-Moyal expansion [15], an evolution equation for the probability distribution function $P(X, l)$ which reads:

$$\frac{\partial}{\partial l}P(X,l) = \sum_{n=1}^{\infty}(-1)^n \frac{\partial^n}{\partial X^n}\left(D_n(X,l)P(X,l)\right). \tag{14}$$

The Kramers-Moyal coefficients $D_n(X, l)$ in Eq. (14) are defined as the limit:

$$D_n(X,l) = \lim_{l'\to l} M_n\left(X, l, l'\right), \tag{15}$$

where the functions $M_n\left(X, l, l'\right)$ are equal, for $l \neq l'$ and up to a multiplicative factor, to the n-th order moment of the transition probability distribution function:

$$M_n\left(X, l, l'\right) = \frac{1}{l - l'}\,\frac{1}{n!}\int (X' - X)^n\, P(X', l'|X, l)\, dX'. \tag{16}$$

In [14], the coefficients $D_n(X, l)$ are equated to numerical values found for $M_n(X, l, l' = l + \delta l)$, $\delta l = 0.04$, below which resolution becomes insufficient. According to this procedure, the second and fourth-order coefficients D_2 and D_4 are found roughly constant, i.e. independent of both variables X and l, with $D_4 \leq 0.05(D_2)^2$, and $D_2 = 0.03 \pm 0.005$. The inequality is interpreted by neglecting the fourth-order term in Eq. (14): $D_4(X, l) = 0$. If $D_4 = 0$, Pawula's theorem [15] then implies that the expansion (14) may be truncated at second order. In particular, $D_3(X, l) = 0$, and Eq. (14) reduces to the Fokker-Planck equation:

$$\frac{\partial}{\partial l}P(X,l) = -\frac{\partial}{\partial X}\left(D_1(X,l)P(X,l)\right) + \frac{\partial^2}{\partial X^2}\left(D_2(X,l)P(X,l)\right), \tag{17}$$

where $D_2(X, l) = D$ is a diffusion constant.

Using the same procedure, the first-order coefficient is found linear in X, with

an approximately scale-independent slope γ. Using at each scale the centered variable $X - \langle X(l) \rangle$, one may write:

$$D_1(X, l) = \gamma(X - \langle X(l) \rangle) + F(l), \tag{18}$$

where $F(l)$ is a (real) function of scale, and $\gamma = 0.21 \pm 0.02$. Eqs. (17)-(18) define an Ornstein-Uhlenbeck process with drift and diffusion coefficients γ and D [15]. The drift coefficient γ, a real number, should not be confused with the drift *term* $D_1(X, l)$, a real function of variables X and l. Note that γ is found positive: the process does not relax to a stationary state for large l.

In [14], Eq. (17) is integrated by assuming that energy does not fluctuate at the largest scale L, as expected in the ideal case of an ensemble of systems supplied with the same power. The corresponding initial condition reads:

$$P(X, l = 0) = \delta \left(X(0) - \ln \epsilon_L \right) \tag{19}$$

The Fokker-Planck equation supplemented with Eq. (19) admits an exact, Gaussian solution:

$$P(X, l) = \frac{1}{\Lambda(l)\sqrt{2\pi}} \exp \left(-\frac{(X - \langle X(l) \rangle)^2}{2\Lambda^2(l)} \right). \tag{20}$$

Similarly to Kolmogorov and Obukhov's model [4], the dissipation exhibits log-normal fluctuations.

Since energy is conserved through the cascade (i.e. $\forall r \in [\eta, L]$, $\langle \epsilon_r \rangle = \langle \epsilon \rangle$), the mean and variance of the Gaussian probability distribution function (20) are simply related by:

$$\langle X(l) \rangle = \langle X(0) \rangle - \Lambda^2(l)/2, \tag{21}$$

in good agreement with experimental data. According to Eq. (19), we postulate that $\langle X(0) \rangle = X(0) = \ln \epsilon_L$. The variance $\Lambda^2(l)$ of the Gaussian solution (20) is a monotonously decreasing function of scale r:

$$\Lambda^2(l) = \frac{D}{\gamma} \left(e^{2\gamma l} - 1 \right) = \frac{D}{\gamma} \left(\left(\frac{L}{r} \right)^{2\gamma} - 1 \right). \tag{22}$$

A consistency condition is:

$$F(l) = \frac{d}{dl} \langle X(l) \rangle = -D e^{2\gamma l}, \tag{23}$$

in good agreement with direct measurements of the first-order Kramers-Moyal coefficient $D_1(X,l)$. Note that Eq. (2) is recovered when the drift coefficient γ cancels, with $\mu = 2D$ and $\Lambda_0^2 = 0$. For small enough scales ($r \ll L$), Eq. (22) reduces to a power-law dependence, in agreement with Castaing's model. In that context, γ was observed to be inversely proportionnal to $\log(Re)$ [10,16].

One may summarise the main result of [14] as follows: an Ornstein-Uhlenbeck process with positive drift coefficient (Eqs. (17)-(18)) gives a simple picture of the scale dependence of energy transfer statistics of a turbulent flow. The validity of this description relies on two assumptions: first that the process is Markov, second that the Kramers-Moyal coefficients of order strictly larger than 2 may be neglected, in particular that $D_3(X,l)$ and $D_4(X,l)$ may be set to zero. The analysis made in [14] suggests that both assumptions are reasonably well-supported by experimental data. However, one may already note that the non-zero, negative skewness of $P(X,l)$ observed in Fig. 1 is not taken into account by the Fokker-Planck model. In what follows, we adopt the complementary perspective provided by a formally equivalent Langevin description in order to better assess the validity of these approximations.

5 A Langevin equation

We will study in this section the energy cascade process from the perspective given by scale-dependent random trajectories of the centered stochastic variable $Y(l)$. A Langevin equation formally equivalent to the Fokker-Planck equation (17) is first introduced in Sec. 5.1. We proceed to measure directly the drift and diffusion coefficients γ and D (Secs. 5.2) by methods which do not involve the computation of Kramers-Moyal coefficients. Predictions involving the two-point correlators of $Y(l)$ are next confronted to experimental data in Sec. 5.3. A definition of the random force is finally introduced in Sec. 5.4, thanks to proper discretisation of the Langevin equation.

5.1 The equivalent Langevin description

Eqs. (17-19) and (23) are mathematically equivalent to the stochastic differential equation [15]:

$$\frac{dY}{dl}(l) = \gamma Y(l) + \sqrt{2D}\,\xi_{\mathrm{FP}}(l) \tag{24}$$

with initial condition $Y(0) = 0$ (note that $F(l) = d\langle X(l)\rangle/dl$). When strict equivalence with the Fokker-Planck equation (17) holds, the random force

$\xi_{\rm FP}(l)$ is a stationary, Gaussian, white noise and the stochastic process is Markov. The two-point correlation function therefore reads:

$$\langle \xi_{\rm FP}(l)\ \xi_{\rm FP}(l')\rangle = \delta(l-l'), \tag{25}$$

and the probability distribution function is a scale-independent Gaussian:

$$P(\xi_{\rm FP}, l) = \frac{1}{\sqrt{2\pi}}\ \exp\left(-\frac{{\xi_{\rm FP}}^2}{2}\right), \tag{26}$$

with mean $\langle \xi_{\rm FP}(l)\rangle = 0$ and variance $\langle \xi_{\rm FP}(l)^2\rangle = 1$.

The linear equation (24) is exactly solvable. Its solution reads:

$$Y(l) = Y(0) + \sqrt{2D}\int_0^l e^{\gamma(l-l')}\ \xi(l')\ {\rm d}l'. \tag{27}$$

Two-point statistics of the process $Y(l)$ can also be calculated when the random force is delta-correlated (Eq. (25)). Assuming that the initial distribution $P(Y,0)$ admits a finite width $\langle Y(0)^2\rangle$, one obtains:

$$\langle Y(l)^2\rangle = \langle Y(0)^2\rangle + \frac{D}{\gamma}\left(e^{2\gamma l} - 1\right). \tag{28}$$

Expression (22) is recovered when $\langle Y(0)^2\rangle = 0$, as expected. Further, we define the normalised scale autocorrelation function of the stochastic process $Y(l)$ by the relation:

$$C_Y(l, \Delta l) = \frac{\langle Y(l)\ Y(l+\Delta l)\rangle}{\langle Y(l)^2\rangle}, \tag{29}$$

where Δl is a positive scale difference. A straightforward calculation leads to:

$$\ln C_Y(l, \Delta l) = \gamma\ \Delta l. \tag{30}$$

Note that expressions (28) and (30) are obtained independently of the functional form of the probability distribution function of the random force.

5.2 Drift and diffusion coefficients

Assuming that the energy cascade process can be described by a Langevin equation such as (24), one would first of all like to check whether this equation

is indeed linear. Since $\langle \xi(l) \rangle = 0$, a straightforward consequence of Eq. (24) is:

$$\left\langle \dot{Y}(l) | Y(l) \right\rangle = \gamma Y(l), \tag{31}$$

where $\dot{Y}(l)$ denotes the derivative of $Y(l)$ with respect to scale. It is easy to see that nonlinear functions of $Y(l)$ in the right hand side of Eq. (24) would also contribute to the the conditional average $\langle \dot{Y}(l) | Y(l) \rangle$. Direct measures of $\langle \dot{Y}(l) | Y(l) \rangle$ are presented in Fig. 2, where the prescriptions detailed in Sec. 3 were used. Within statistical error, the conditional average $\langle \dot{Y}(l) | Y(l) \rangle$ is indeed proportional to $Y(l)$, even though a small, possibly cubic contribution appears at small scales for (rare) large negative values of the variable $Y(l)$. This observation confirms the linearity of the relevant Langevin equation. However, the corresponding slope γ seems to be an increasing function of scale.

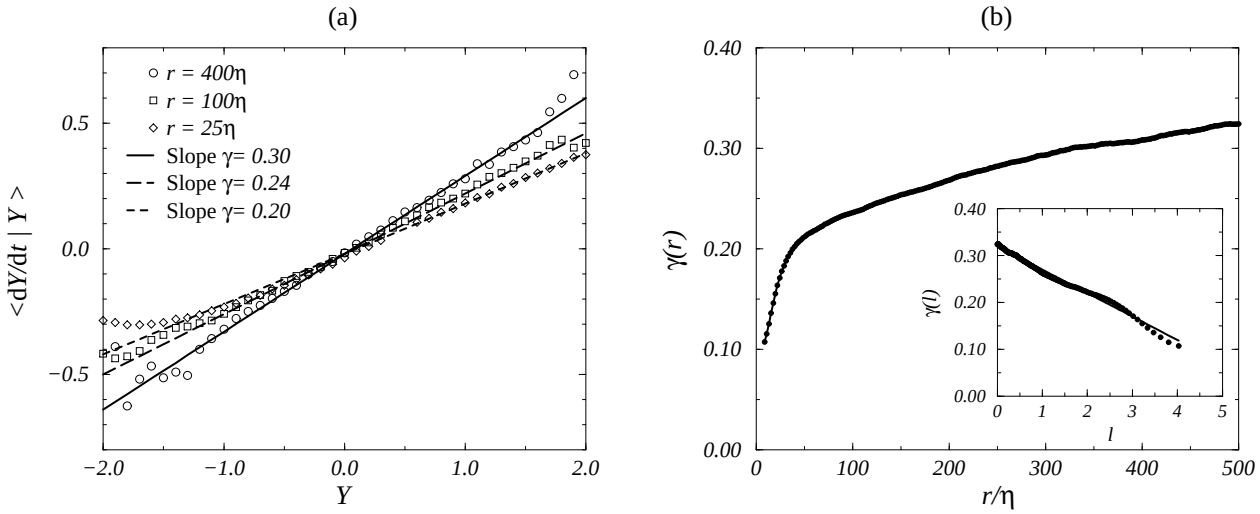

Fig. 2. Measure of the drift coefficient $\gamma(l)$. Graph (a): plot of the conditional average $\langle \dot{Y}(l) | Y(l) \rangle$ vs. $Y(l)$, estimated at scales $r = 25\eta, 100\eta$ and 400η. Straight lines of slope 0.20, 0.24 and 0.30 are drawn to guide the eye. Graph (b): plot of $\gamma(r)$, as defined in Eq. (33), versus scale r/η. Statistical error is of the order of a few percent in relative value. Inset: log-lin plot of the same data ($l = \ln(L/r)$). The straight line corresponds to $\gamma(l) = 0.32 - 0.05\, l$.

Using Eq. (31) to obtain quantitatively accurate estimates of $\gamma(l)$ is rather costly numerically. We will turn to a simpler method, which turns out to yield consistent estimates. Implicit in Eq. (24) is the assumption that the random force $\xi_{\rm FP}(l)$ is statistically independent from the stochastic variable $Y(l)$ at all scales l:

$$\langle Y(l)\, \xi_{\rm FP}(l) \rangle = 0. \tag{32}$$

Upon multiplying both sides of the Langevin equation (24) by $Y(l)$, ensemble-averaging, and using Eq. (32), one easily obtains:

$$\gamma(l) = \frac{\langle \dot{Y}(l)\, Y(l) \rangle}{\langle Y(l)^2 \rangle}, \tag{33}$$

where the drift coefficient $\gamma(l)$ is a priori a function of scale. Fig. 2.b shows that $\gamma(l)$, as estimated thanks to Eq. (33), is indeed a slowly varying function of scale. The order of magnitude is however the same as that of the (constant) value advocated in [14] (0.21 ± 0.02). This method appears to be more sensitive than direct calculations of the Kramers-Moyal coefficients.

We would like to emphasise that: (i) Eqs. (31) and (33) yield mutually consistent estimates of $\gamma(l)$; (ii) the normalised cross-correlation function $C_{Y\xi}(r)$, defined as:

$$C_{Y\xi}(r) = \frac{\langle Y(r)\, \xi(r) \rangle}{Y_{\rm rms}(r)\, \xi_{\rm rms}(r)}, \tag{34}$$

is indeed close to zero (in practice of the order of 10^{-2}) when the random force $\xi(l)$ is calculated thanks to Eq. (43) for constant drift and diffusion coefficients, e.g. $\gamma(l) = \gamma = 0.21$ and $D(l) = D = 0.03$.

As shown in the inset of Fig. 2, the scale dependence of the drift coefficient is well described by a linear function of l over the whole range of relevant scales. Introducing a factor 2 for convenience, we write:

$$\gamma(l) = \gamma_0 - 2\gamma_1 l. \tag{35}$$

Our estimates of the constants γ_0 and γ_1 are $\gamma_0 = 0.32 \pm 0.03$ and $\gamma_1 = 0.025 \pm 0.003$. The error bars take into account both statistical error and the uncertainty deriving from the existence of other possible choices of the discretisation steps δr and $\delta x'$. Note that the drift coefficient is positive for all physically relevant scales: Eq. (35) yields $\gamma(r = \eta) = 0.01 > 0$.

Assume now that the second-order Kramers-Moyal coefficient $D_2(X, l)$ is independent of X, and reduces to a (possibly scale-dependent) diffusion coefficient $D(l)$. According to Eq. (24), this coefficient may then be defined as:

$$2D(l) = \left\langle \left(\frac{dY}{dl}(l) - \gamma(l)\, Y(l) \right)^2 \right\rangle, \tag{36}$$

where the variance of the random force is set to unity: $\langle \xi(l)^2 \rangle = 1$. Using Eq. (36), where $\gamma(l)$ is evaluated thanks to Eq. (33), we find a finite, *scale-*

dependent, monotonously decreasing coefficient diffusion $D(r)$ (as a function of the physical scale r, see Fig. 3). The order of magnitude is consistent with that of the constant value advocated in [14] ($D = 0.03 \pm 0.01$). An excellent fit of the data is given by the expression:

$$D(l) = D_0 \, e^{2\,\delta\,l}, \tag{37}$$

with $D_0 = 0.01 \pm 0.005$ and $\delta = 0.40 \pm 0.01$ (see the inset of Fig. 3), except at scales r close to the dissipation scale η.

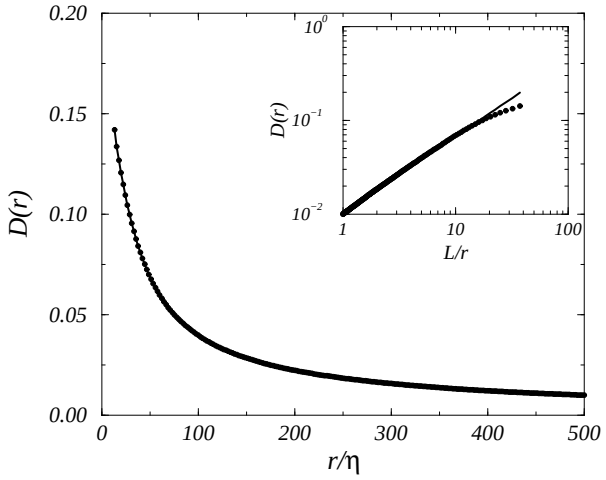

Fig. 3. Graph of the diffusion coefficient $D(l)$ (as defined in Eq. (36)) versus scale r/η. Statistical errors are smaller than the width of the symbols used. Inset: same data in log-log scale. The straight line corresponds to the scaling law $D(r) = 0.01(L/r)^{0.4}$.

We have shown in this section that the drift and diffusion coefficients, when measured according to Eqs. (33) and (36), are in fact not independent of the scale l. Since this scale-dependence cannot be attributed to, say, statistical errors, it becomes essential to understand to what extent the coefficients $\gamma(l)$ and $D(l)$ may be approximated by constant coefficients, as has been advocated in [14]. This is the goal of the next section, where predictions concerning the two-point statistics of $Y(l)$ will be confronted to experimental data for both scale-dependent and constant coefficients.

5.3 Two predictions

Instead of Eq. (24), we now use the following Langevin equation as our starting point:

$$\frac{dY}{dl}(l) = \gamma(l)Y(l) + \sqrt{2D(l)}\,\xi(l), \tag{38}$$

where the functions $\gamma(l)$ and $D(l)$ are given by Eqs. (35) and (37) respectively. The solution of Eq. (38) reads:

$$Y(l) = e^{\gamma_0 l - \gamma_1 l^2}\left(Y(0) + \sqrt{2D_0}\int_0^l e^{(\delta-\gamma_0)l' + \gamma_1 l'^2}\xi(l')\mathrm{d}l'\right). \tag{39}$$

Assuming that the random force $\xi(l)$ is delta-correlated, we obtain the following expression of the variance of $Y(l)$:

$$\langle Y(l)^2\rangle = e^{2\gamma_0 l - 2\gamma_1 l^2}\left(\langle Y(0)^2\rangle + 2D_0\int_0^l e^{2(\delta-\gamma_0)l' + 2\gamma_1 l'^2}\mathrm{d}l'\right) \tag{40}$$

for an initial width $\langle Y(0)^2\rangle$. The normalised scale autocorrelation function of the stochastic process $Y(l)$ then reads:

$$\ln C_Y(l,\Delta l) = (\gamma_0 - 2\gamma_1 l)\Delta l - \gamma_1(\Delta l)^2. \tag{41}$$

In Fig. 4.a, we compare the scale dependence of $\langle Y(l)^2\rangle$, as obtained from experimental data, with predictions (28) and (40). The initial value is set to $\langle Y(0)^2\rangle = 0.23$. We use the following numerical values: $\gamma = 0.21$ (Eq. (28)), $\gamma_0 = 0.32$, $\gamma_1 = 0.025$, $D_0 = 0.01$, $\delta = 0.40$ (Eq. (40)). We find that Eq. (40), *not* Eq. (28), fits experimental data extremely well. A small deviation is observed only for scales smaller than $r = 25\eta$ ($l \geq 3.0$), where the diffusion coefficient $D(r)$ deviates from the scaling law (37) (see Fig. 3). This first result suggests that approximating the drift and diffusion coefficients to a constant value is inappropriate.

Fig. 4.b shows the measured scale autocorrelation functions $C_Y(l,\Delta l)$. Again, the linear growth predicted by Eq. (30) is not observed. However, the following features of the scale-dependence of $C_Y(l,\Delta l)$ are reproduced by Eq. (41) at a qualitative level. The autocorrelation function is a function of both l and Δl. For all (fixed) values of l, its logarithm first grows with Δl before reaching a maximum and eventually decaying. The tangent at $\Delta l = 0$ is smaller than $\gamma_0 =$

0.32. However, quantitative agreement is still lacking, for instance concerning the location of the maximum of $C_Y(l, \Delta l)$, as well as the exact dependence in Δl. We will show in Sec. 6 that, as one would now expect, a δ-function is indeed a good approximation of the autocorrelation function of the noise $C_\xi(l, \Delta l)$, as shown by comparing the correlation scale of C_ξ to the evolution scale of C_Y. We therefore believe that the quantitative discrepancy observed between the prediction (41) and experimental data should be attributed to the approximation made when fitting $\gamma(r)$ by a logarithmic function of scale. In particular, the oscillations apparent in the inset of Fig. 2 for large l do not seem to be statistical fluctuations, and should therefore be taken into account when computing $C_Y(l, \Delta l)$.

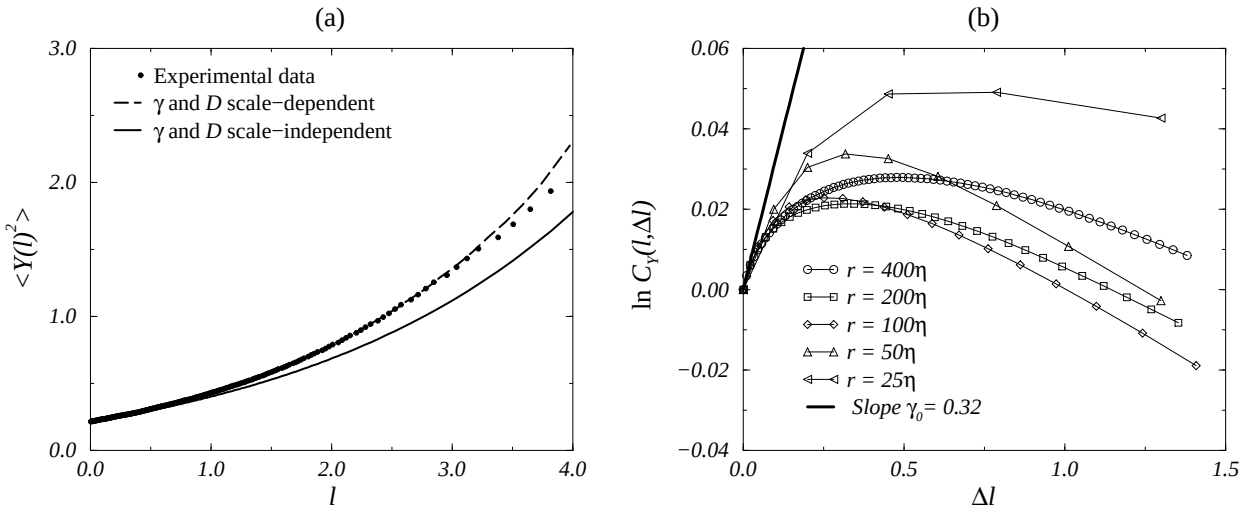

Fig. 4. Graph (a): variance of $Y(l)$. The statistical error on experimental data is smaller than the width of symbols. The prediction obtained in the case of scale-dependent coefficients (Eq. (40), dashed line) is indistinguishable from experimental data in the interval $0 \leq l \leq 3$. See text for the numerical values used in the calculation of $\langle Y(l)^2 \rangle$. Graph (b): lin-log plot of the scale autocorrelation functions $C_Y(l, \Delta l)$ vs. the scale difference Δl, for scales l ranging from $l = 25\eta$ to $l = 400\eta$. A straight line with slope γ_0 is also shown for comparison with the behaviour expected in the vicinity of $\Delta l = 0$ in the case of scale-dependent drift and diffusion coefficients (Eq. (41)).

In conclusion, $\gamma(l)$ and $D(l)$ should not be approximated to a constant value. Further, the functional dependence given by Eqs. (35) and (37) is consistent with experimentally obtained two-point correlators of the process $Y(l)$, qualitatively only for the autocorrelation function $C_Y(l, \Delta l)$, and quantitatively for the variance $\langle Y(l)^2 \rangle$.

5.4 Discretisation scheme

In the following, we will consider the Langevin equation (38), where $\gamma(l)$ and $D(l)$ are defined by Eqs. (33) and (36) respectively. Provided that the noise term $\xi(t)$ is Gaussian, stationary, and delta-correlated, this equation is formally equivalent to a Fokker-Planck equation such as Eq. (17), with scale-dependent drift and diffusion coefficients. As before, this Fokker-Planck equation admits a Gaussian solution, the variance of which is given by Eq. (40.

The stochastic differential equation (38) may be discretised according to the following first-order scheme [15]:

$$Y\left(l+\delta l\right) - Y(l) = \gamma(l)\; Y(l)\; \delta l + \sqrt{2\; D(l)\; \delta l}\; \xi(l). \tag{42}$$

In the following, we will use Eq. (42) as an operational definition of the driving random force:

$$\xi(l) \equiv \frac{1}{\sqrt{2\; D(l)\; \delta l}} \left(Y(l+\delta l) - Y(l) - \gamma(l)\; Y(l)\; \delta l\right). \tag{43}$$

By construction, $\xi(l)$ is a centered stochastic variable at all scales l: $\langle \xi(l) \rangle = 0$, with unit variance $\langle \xi(l)^2 \rangle = 1$.

In Secs. 6 and 7, we will respectively test the Markov and Gaussian nature of the stochastic process defined by Eq. (38).

6 A Markov process

In this section, we further investigate the validity of Eq. (38) by turning to the dynamics of the process, and in particular to two-point scale autocorrelation functions.

Due to the viscosity of the fluid, the velocity field of a turbulent flow remains differentiable. The energy cascade cannot be perfectly represented by a Markov process: the process $\xi(l)$ must also be differentiable, and can therefore not be δ-correlated. Its (normalised) two-point scale autocorrelation function is defined as:

$$C_\xi(l,l') = \langle \xi(l)\; \xi(l') \rangle\,. \tag{44}$$

Fig. 5.a shows that the scale dependence of $C_\xi(l,l')$ cannot be reduced to the

form $C_\xi(l'-l)$. The process is thus instationary in terms of the scale variable l. One may however write without loss of generality:

$$C_\xi(l,l') = C_\xi(l,\Delta l), \tag{45}$$

where $\Delta l = l' - l$ is set positive by convention. Further, correlations of the random force differ from the ideal case (Eq. (25)): the autocorrelation scale $\tau(l)$ is non-zero, its numerical value depends on scale l. Even though the scale autocorrelation function decays approximately exponentially over roughly one decade, we choose to evaluate the characteristic correlation scale $\tau(l)$ from the expression :

$$\tau(l) = \int_0^\infty C_\xi(l,\Delta l)\,\mathrm{d}\Delta l. \tag{46}$$

We checked that this particular choice does not affect our conclusions.

The autocorrelation scale $\tau(l)$ is a quantitative measure of the departure from the Markov approximation. At a given scale l, the scale $\tau(l)$ marks the limit below which the stochastic cascade process becomes smooth. In this sense, the (measurable) scale $\tau(l)$ is the elementary step of the energy cascade.

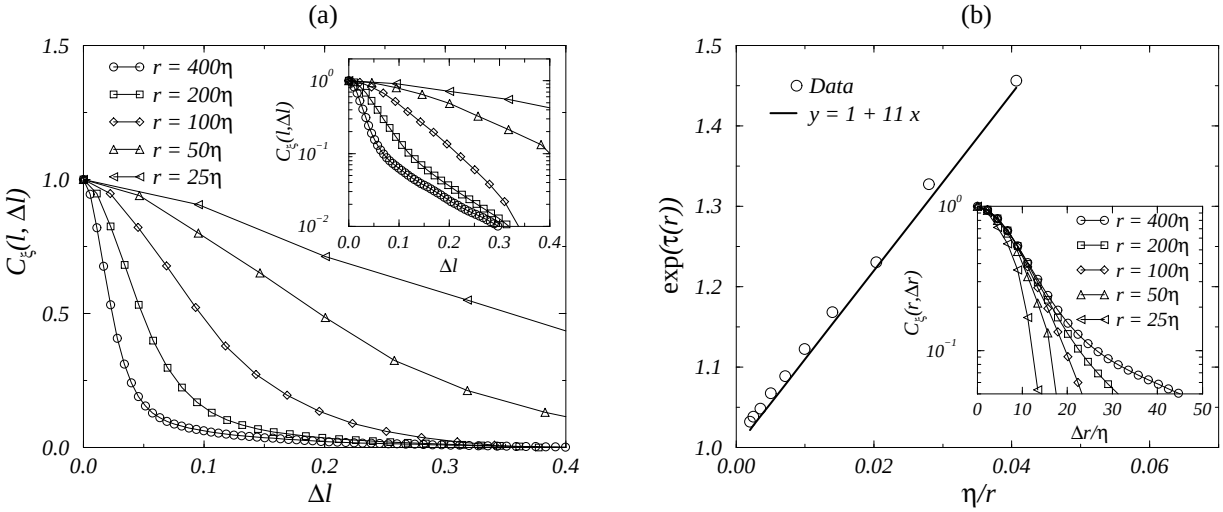

Fig. 5. Graph (a): scale autocorrelation function $C_\xi(l,\Delta l)$ of the random force $\xi(l)$ for scales $r = L\exp(-l)$ ranging between $r = 25\eta$ and $r = 400\eta$. The statistical error is smaller than the width of symbols. Inset: lin-log plot of the same curves. Graph(b): scale-dependence of the autocorrelation scale $\tau(r)$. Inset: same graph as (a), represented as a function of the physical scale r.

Eq. (46) yields numerical values ranging between $\tau = 0.37$ when $r = 25\eta$ and $\tau = 0.03$ when $r = L = 500\eta$. Fig. 5.b shows that the scale-dependence of $\tau(l)$

may be fitted by the expression:

$$\tau(r) = \ln\left(\frac{r + r_0}{r}\right), \tag{47}$$

for a numerical value of r_0 close to 11 η. In other words, the instationarity observed at the level of autocorrelation functions (Fig. 5.a) is mostly due to the change of variable $l = \ln(L/r)$. This is confirmed by the insert of Fig. 5.b, where the autocorrelation functions C_ξ are plotted with respect to the physical scale difference Δr: the first decade of decay is characterised at all scales by a slope roughly equal to $1/r_0$. In terms of the scale variable r, the elementary cascade step may simply be defined as r_0, of the order of Kolmogorov's scale η.

The characteristic evolution scale of the random process $Y(l)$ at scale l is given by the inverse drift coefficient $1/\gamma(l)$ (cf. Eq. (38)). The product $\gamma(r)\tau(r)$ is a monotonically decreasing function of scale r, with $\gamma(25\eta)\tau(25\eta) = 0.06$ and $\gamma(L)\tau(L) = 0.01$. In the range of scales $25\eta \leq r \leq 500\eta$ at least, one finds that:

$$\tau(l) \ll \frac{1}{\gamma(l)}, \tag{48}$$

by more than one order of magnitude. Although the correlation scale $\tau(l)$ is non-zero, the random process $Y(l)$ is therefore effectively Markov. Moreover, the product $\gamma(r)\tau(r)$, as defined by Eqs. (35) and (47), admits an absolute maximum close to 0.1 in the vicinity of $r \sim 5\eta$. Assuming that Eqs. (35) and (47) faithfully describe the scale dependence of $\gamma(l)$ and $\tau(l)$ down to the smallest scales, this implies that the energy cascade is always a Markov stochastic process for scales larger than η.

7 A non-gaussian random force

In this section, we investigate the validity of Eq. (26) by evaluating the probability distribution function $P(\xi, l)$ of the random force ξ at scale l.

7.1 A typical realisation of the process $\xi(l)$

A typical realisation of the random processes $Y(l)$ and $\xi(l)$ is presented in Fig. 6. The dynamics of $Y(l)$ is generally dominated by the deterministic part of Eq. (38). Long periods of quasi-exponential growth controlled by the drift

coefficient $\gamma > 0$ are perturbed by small deviations due to the random force $\xi(l)$. This regime is interrupted infrequently by sharp drops, corresponding to large negative excursions of the random force. This suggests that the probability distribution function of ξ is strongly skewed, in contrast with the Gaussian prediction. Accessible values of $\xi(l)$ also seem to be bounded from above.

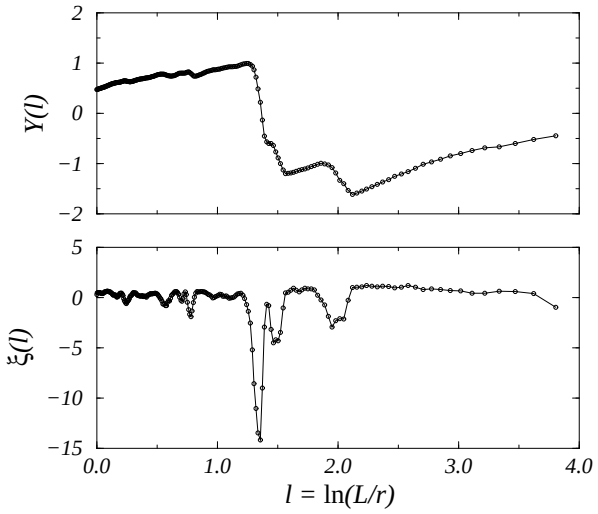

Fig. 6. A typical random trajectory of the stochastic processes $Y(l)$ and $\xi(l)$. Note that $Y(0)$ is not equal to zero.

7.2 Probability distribution function of the random force

As shown in Fig. 7, the probability distribution function $P(\xi, r)$ of the random force ξ at scale r is markedly different from the Gaussian prediction (Eq. (26)): the skewness factor of $P(\xi, r)$ is indeed negative. The shape of $P(\xi, r)$ depends on scale r: this is consistent with the instationary behaviour of autocorrelation functions (cf. Sec. 6). Even though Gaussian-like, rapid decay of $P(\xi, r)$ is observed for $\xi > 0$, the probability of large negative deviations is much larger than that predicted for a Gaussian process. This long tail can be fitted with reasonable accuracy either by a log-normal or by a stretched-exponential functional form.

The Gaussian-like decay of $P(\xi)$ for positive values of the random force may be understood as follows. The definition of ϵ_r as a sum of non-negative quantities (Eq. (4)) implies that:

$$r' \, \epsilon_{r'} < r \, \epsilon_r, \; \forall \, r' < r. \tag{49}$$

The process $X(l)$ can only adopt values such that:

$$X(l') - X(l) < l' - l, \ \forall \ l' > l. \tag{50}$$

Taking the appropriate limit, one obtains:

$$\dot{Y}(l) \leq 1 - \frac{\mathrm{d}}{\mathrm{d}l}\langle X(l)\rangle. \tag{51}$$

The random force ξ is defined as the difference of the two random variables $\dot{Y}$ and Y, where $\dot{Y}$ admits an upper bound and the fluctuations of Y are nearly Gaussian: the tail of $P(\xi, l)$ is thus expected to be Gaussian-like for positive values of the random force ξ.

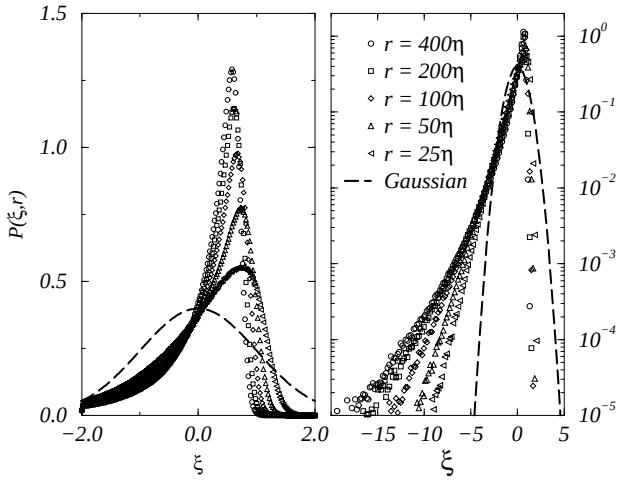

Fig. 7. Probability distribution functions $P(\xi, r)$ of the random force ξ for scales r ranging from $r = 25\eta$ to $r = 400\eta$ in lin-lin (left-hand side) and lin-log (right-hand side) plots. The dashed line is drawn for comparison with the Gaussian prediction derived from the Fokker-Planck model.

At a qualitative level, the asymmetry of the probability distribution function of ξ is readily understood if one remembers that $P(Y, r)$ is also asymmetrical, as seen in Fig. 1. The solution of a linear stochastic evolution equation with Gaussian random driving is symmetrical. Conversely, the skewness of the variable $Y(l)$ points at the necessity of corrections to the Fokker-Planck model. The dominant one is expected to stem from the third-order coefficient D_3. Non-zero n-th order coefficients M_n translate into deviations of the n-point correlators of the random force $\xi(l)$ from their Gaussian form. In particular, a non-zero value of D_3 translates into a non-zero skewness, as observed here. The asymmetry of $P(Y, r)$ is weak, as quantified by the small value of the parameter $|D_3(l)|/D(l)^{3/2}$, which we found smaller than 10^{-1} at all scales.

Intermittency of fully-developed turbulent flows is often characterised by the presence of large excursions of the (positive) local dissipation rate $\epsilon(x) = 15\nu(dv/dx)^2$ far above its mean value. We believe that these rare events also correspond to large negative deviations of the process $\xi(l)$. The dissipation rate $\epsilon_r(x)$ at location x is defined as the spatial average of $\epsilon(x)$ over an interval of length r (Eq. (4)). The location x being fixed, $\epsilon_r(x)$ is a monotonously decreasing function of scale r when the integral of $\epsilon(x)$ over an interval of length r grows more slowly than r, i.e. when fluctuations of $\epsilon(x)$ are weak enough. This case corresponds to the periods of quasi-exponential growth of $Y(l)$ in Fig.6. Assume now that a sharp increase of $\epsilon(x)$ takes place close to $x^* = x + r^*/2$. Close to r^*, the value of $\epsilon_r(x)$ will increase sharply: $\epsilon_{r^*+\delta r}(x) \gg \epsilon_{r^*-\delta r}(x)$, corresponding to a large positive value of the scale derivative $\partial\epsilon_r(x)/\partial r_{|r=r^*}$. Since the logarithmic scale l is a monotonously decreasing function of the physical scale r, this shows that intermittent bursts of $\epsilon(x)$ do indeed correspond to sharp and localised drops of $Y(l)$. In other words, the asymmetry of $P(\xi, r)$ expresses the intermittent character of the local dissipation field.

However, the definition of ϵ_r as the averaged dissipation rate over a segment of length r is to some extent arbitrary. The amplitude of intermittent events, as quantified by the value of $\xi(l^*)$ close to a large deviation of the local dissipation rate $\epsilon(x^*)$, may depend sharply on the precise definition of the averaging procedure which leads to $\epsilon_r(x)$. In this sense, we conjecture that the precise numerical value of, e.g., the skewness coefficient of $P(\xi, r)$ is in fact not relevant to the description of the physical cascade process, since it may depend on arbitrary features of the analysis method, such as the choice of an averaging window in Eq. (4).

8 Discussion

Following [14], we have found additional evidence that the energy cascade of a turbulent flow at high Reynolds number is well described by a continuous stochastic process of Ornstein-Uhlenbeck type. We also clarified the validity of a number of approximations made in [14].

Defining the stochastic process $Y(l)$ as the centered variable $\ln \epsilon_r - \langle \ln \epsilon_r \rangle$ at scale $l = \ln(L/r)$, the relevant Langevin equation is linear, and reads:

$$\frac{dY}{dl}(l) = \gamma(l)Y(l) + \sqrt{2D(l)}\,\xi(l). \tag{52}$$

We found that the scale-dependence of the drift and diffusion coefficients $\gamma(l)$ and $D(l)$, as evaluated directly from experimental data by methods independent from those used in [14], is well described by the following functional

forms:

$$\begin{aligned} \gamma(l) &= \gamma_0 - \gamma_1\, l, \\ D(l) &= D_0\, e^{2\,\delta\, l}, \end{aligned} \tag{53}$$

where $\gamma_0 = 0.32 \pm 0.03$, $\gamma_1 = 0.025 \pm 0.003$, $D_0 = 0.01 \pm 0.005$, and $\delta = 0.40 \pm 0.01$ are positive constants. The (exact) solution of Eqs. (52)-(53) is in good agreement with experimental data at the level of two-point correlators of the stochastic variable $Y(l)$. Further, we have shown that the drift and diffusion coefficients cannot be approximated by constant values if one wants to preserve this agreement.

The main characteristics of the random force $\xi(l)$ have been determined directly from experimental data. We have checked that the process is Markov at all scales l, since scale autocorrelation functions of the random force decay rapidly on a characteristic autocorrelation scale $\tau(l)$ much smaller than the typical evolution scale $1/\gamma(l)$ of the process. This is perhaps our most important result: the Langevin equation (52) defines a driving random force $\xi(l)$ which respects the Markov hypothesis. Previous work [14] only provided evidence for the validity of a necessary condition for the additive process (38) to be Markov. The autocorrelation scale $\tau(l)$ is the elementary step of the cascade process. It depends on the physical scale r as $\tau(l) = \ln\left((r + r_0)/r\right)$, where r_0 is of the order of Kolmogorov's scale η.

Finally, our analysis of experimental data shows that the probability distribution function of the random force $\xi(l)$ is strongly non-Gaussian, and exhibits a long tail for negative noise (see Fig. 1). These rare, but intense deviations are correlated with large positive values of the scale derivative $\partial\epsilon_r/\partial r$. For a linear equation such as (38), the non-zero skewness of $P(\xi, l)$ translates into an asymmetrical solution $P(Y, l)$, in qualitative agreement with observation. This deviation from the simple Ornstein-Uhlenbeck picture is equivalent to a correction to log-normal statistics for the energy dissipation rate ϵ_r. Within the Fokker-Planck description, the corresponding leading-order correction is the third-order term of the Kramers-Moyal expansion (Eq. (14)), with a non-zero, scale-dependent coefficient $D_3(l)$. This correction is weak, as quantified by the value of the ratio $|D_3(l)|/D^{3/2}$, smaller than 10^{-1} at all scales. This correction is made at the expense of the solvability of our model.

Two comments are in order. First, this stochastic description of the energy cascade (including the Markov property) applies to all scales, from the integral scale L down to the dissipation scale η. The distinction commonly observed between dissipative and inertial sub-range statistics of, e.g., turbulent velocity and passive scalar density fields [1], appears to be irrelevant in the case of the energy dissipation rate. Second, all known multiplicative models of the

cascade use, at least to our knowledge, a scale-independent discretisation step such as $\ln 2$. Although natural from a mathematical viewpoint, this choice overlooks the scale-dependence of $\tau(l)$ observed here, and may thus not be appropriate on physical grounds. The choice of the discretization step of a discrete stochastic model of the energy cascade is not meaningless.

We would now like to emphasise that observations reported in this work stem from the analysis of one turbulent velocity signal, recorded in a particular realisation of a jet flow at a given value of the Reynolds number. One would of course like to know to what extent the Langevin equation (52) is a universal description of the energy cascade. Preliminary studies have already shown that the statistical properties of the processes $\xi(l)$ and $Y(l)$ are qualitatively similar to those discussed here for other values of the Reynolds number [21]. Further, a number of adimensional quantifiers of the energy cascade have been introduced at a rather formal level ($\gamma(l)$, $D(l)$, etc.). One would like to understand their physical meaning, as indicated by, e.g., a possible dependence on the physical properties of the fluid and the Reynolds number, and in particular to elucidate their behaviour in the limit of large Re. Conversely, it is also essential to check whether some of our results, such as the numerical value of, say, the skewness of $P(\xi, r)$, may not be artefacts of the data processing method. These important points are currently being considered, thanks to the analysis of the velocity fields of other turbulent flows.

Interestingly, the existence of a stochastic evolution equation in scale allows, at least in principle, to reconstruct by simple integration the small scale statistics of the dissipation field from spatial fluctuations observed at larger scale. We therefore believe that this description of the energy cascade process may prove useful, as a model of the small scale fluctuations, in the context of large eddy simulations where only the larger scales of a flow are usually resolved.

Acknowledgements

The authors would like to thank Yoshiki Kuramoto for his support as well as for many insightful comments, Jean-François Pinton for a critical reading of the manuscript, and Bernard Castaing for a useful discussion. The warm hospitality of Kyoto university, Tohoku university and Ecole Normale Supérieure de Lyon is gratefully acknowledged.

References

[1] A.S. Monin and A.M. Yaglom, *Statistical Fluid Mechanics* (MIT Press, Cambridge, MA, 1975); U. Frisch, *Turbulence* (Cambridge University Press, Cambridge, 1995).

[2] M. Nelkin, Adv. in Physics **43**, 143 (1994); K.R. Sreenivasan and R.A. Antonia, Ann. Rev. of Fluid Mech. **29**, 435 (1997).

[3] A.N. Kolmogorov, Dokl. Akad. Nauk. SSSR **30**, 299 (1941); **32**, 19 (1941).

[4] A.M. Obukhov, J. Fluid Mech. **13**, 77 (1962); A.N. Kolmogorov, J. Fluid Mech. **13**, 82 (1962).

[5] R.W. Stewart, J.R. Wilson and R.W. Burling, J. Fluid Mech. **41**, 141 (1970).

[6] L.-P. Wang, S. Chen, J.G. Brasseur and J.C. Wyngaard, J. Fluid Mech. **309**, 113 (1996).

[7] A.S. Gurvich and A.M. Yaglom, Phys. Fluids **10**, 559 (1967).

[8] B. Mandelbrot, J. Fluid Mech. **62**, 331 (1974).

[9] K.R. Sreenivasan and G. Stolovitzky, J. Stat. Phys. **78**, 311 (1995); G. Pedrizzetti, E.A. Novikov and A.A. Praskovsky, Phys. Rev. E **53**, 475 (1996); M. Nelkin and G. Stolovitzky, Phys. Rev E **54**, 5100 (1996).

[10] B. Castaing, Y. Gagne and E. Hopfinger, Physica D **46**, 177 (1990).

[11] A. Arnéodo, J.F. Muzy and S.G. Roux, J. Phys. II (France) **7**, 363 (1997); A. Arnéodo, S. Manneville and J.F. Muzy, Eur. Phys. J. B **1**, 129 (1998).

[12] S.A. Orszag, Phys. Fluids **13**, 2211 (1970); E.A. Novikov, Prikl. Math. Mech. **35**, 266 (1971).

[13] R. Friedrich and J. Peinke, Physica D **102**, 147 (1997); Phys. Rev. Lett. **78**, 863 (1997); R. Friedrich, J. Zeller and J. Peinke, Europhysics Lett. **41**, 153 (1998).

[14] A. Naert, R. Friedrich and J. Peinke, Phys. Rev. E. **56**, 6719 (1997).

[15] H. Risken, *The Fokker-Planck Equation* (Springer-Verlag, Berlin, 1984).

[16] B. Chabaud, A. Naert, J. Peinke, F. Chillà, B. Castaing and B. Hébral, Phys. Rev. Lett. **73**, 3227 (1994).

[17] B. Castaing, B. Chabaud, F. Chillà, B. Hébral, A. Naert and J. Peinke, J. Phys. III (France) **4**, 671 (1994).

[18] A. Naert, Ph.D. thesis, Université Joseph Fourier, Grenoble, 1995 (unpublished).

[19] J.-F. Pinton and R. Labbé, J. Phys. II (France) **4**, 1461 (1994).

[20] H. Kahalerras, Y. Malecot, Y. Gagne and B. Castaing, Phys. Fluids **10**, 910 (1998).

[21] A. Naert and P. Marcq, in preparation.